
Article:
Boston, R, Foeller, PY, Sinclair, DC et al. (2016) Synthesis of Barium Titanate Using Deep Eutectic Solvents. Inorganic Chemistry, 56 (1). pp. 542-547. ISSN: 0020-1669

https://doi.org/10.1021/acs.inorgchem.6b02432

Synthesis of barium titanate using deep eutectic solvents

Rebecca Boston, Philip Y. Foeller, Derek C. Sinclair and Ian M. Reaney*

Dr. R. Boston, P. Y. Foeller, Prof. D. C. Sinclair, Prof. I. M. Reaney
Department of Materials Science and Engineering, Sir Robert Hadfield Building, Mappin Street, University of Sheffield, Sheffield, S1 3JD, UK
E-mail: r.boston@sheffield.ac.uk

Abstract: Novel synthetic routes to prepare functional oxides at lower temperatures are an increasingly important area of research. Many of these synthetic routes, however, use water as the solvent and rely on dissolution of the precursors, precluding their use with, for example, titanates. Here we present a low cost solvent system as a means to rapidly create phase-pure ferroelectric barium titanate using a choline chloride-malonic acid deep eutectic solvent. This solvent is compatible with alkoxide precursors and allows for the rapid synthesis of nanoscale barium titanate powders at 950 °C. The phase and morphology were determined, along with investigation of the synthetic pathway, with the reaction proceeding via $BaCl_2$ and TiO_2 intermediates. The powders were also used to create sintered ceramics, which exhibit a permittivity maximum corresponding to a tetragonal-cubic transition at 112 °C, as opposed to the more conventional temperature of ~ 120 °C. The lower-than-expected value for the ferro- to para-electric phase transition is likely due to undetectable levels of contaminants.

Keywords: $BaTiO_3$; processing; solvent templating; synthetic pathway

1. Introduction

Ferroelectric barium titanate has the perovskite crystal structure and is one of the most ubiquitous and highly studied electroceramics. It exhibits high room temperature permittivity (~ 1000 – 3000) and a sequence of phase transitions from cubic - tetragonal – orthorhombic – rhombohedral as a function of decreasing temperature.[1-3] Its high permittivity, coupled with temperature stability through the use of suitable dopants, make $BaTiO_3$ an excellent candidate for the fabrication of multilayer capacitors.[4-7] More recently it has received renewed interest as the basis for the fabrication of lead-free piezoelectric devices.[8]

Traditionally, oxide-based electroceramics such as $BaTiO_3$ have been made *via* solid-state synthesis,[9] which whilst reliable, suffers from several inherent drawbacks. Solid-state synthesis is slow, resulting from relatively long diffusion distances (typically on the order of the particle size of the raw materials) and often suffers from the formation of recalcitrant intermediate phases which are difficult to eliminate in a single or two-step heat treatment.[10] This diffusion-limited compositional heterogeneity can also lead to local variations in functional properties[11] and in many cases the formation of core-shell structures[12] which may or may not be desirable, depending on the target application. Solid-state synthesis also offers little in the way of size or morphological control in the final product.[13] This lack of control means that potential improvements to performance which could be made through the use of structure-function relationships cannot be easily accessed. As such, new, low-temperature, more flexible synthesis routes are an important area of research. Additionally, the advent of the Cold Sintering Process,[14] which is kindling a revolution in processing technology, relies on nanoscale oxides, and as such, the low cost, high volume production of these in a wide variety of materials will become increasingly important.

There have been many schemes to produce nanoscale electroceramic oxides using non-solid-state routes. Of these, hydrothermal and sol-gel are the most widely recognised.[15-17] These

wet chemical syntheses have the advantage over solid-state routes as they start from aqueous or liquid precursor materials and generally result in a homogeneous product. In many cases these products also form more rapidly or at lower temperatures than solid-state synthesis, making them potentially attractive for industrial applications; however, they require costly high pressure vessels and are therefore generally not scalable beyond small volume application. To circumvent many of these issues, biological templates have been used to direct structure in oxides as they form.[18-20] Whilst powerful, this technique suffers from an inherent drawback that water-soluble, low pH precursors must be used, restricting the number of materials which can be made using biotemplates. This requirement rules out, for example, titanates, which form the basis of many technologically interesting oxides. As such, alternative, water-free solvent systems are required which can either be used as small molecule templates to form nanoscale products, or can be combined with biotemplates to recover their structural directing properties.

Recently, ionic liquids (ILs) such as 1-ethyl 3-methyl imidazolium acetate have been shown to act as templates for complex oxides,[21] sometimes with an added biotemplate to further direct the structure of the final product. These synthesis methods are able to utilise water-insoluble templates or precursors such as cellulose or niobium ethoxide, [21] opening up new possible candidates for the rapidly emerging biotemplating field. One drawback of ILs in this capacity is the associated cost, particularly as the IL is lost during synthesis. Deep eutectic solvents (DESs)[22-23] are a cheap and easily-produced form of IL, formed by the concurrent melting of two simple organic species, which, once molten, exhibit a suppressed melting point. Choline chloride and malonic acid, for example, both have melting points around 80 °C but when melted together solidify at 10 °C.[24] Whilst in the molten state, DESs can dissolve metal salts and/or chelate metal cations in a similar manner to that observed in biotemplated[25] or ionic liquid syntheses.[21,26] DESs can therefore provide the same spatial separation during processing, without the need for an aqueous environment, and at a lower cost than for many standard ILs.

DESs are gaining popularity for applications as they can be used as solvents in electrochemical deposition for metal alloys,[24] or as a means of dissolving metals or metal oxides out of a wider bulk,[27] however they have never been used as a direct means of metal oxide synthesis or templating. Here, we present a novel synthetic method for the production of gram-quantities of nanoscale barium titanate ($BaTiO_3$) powders using a choline chloride and malonic acid DES.

2. Experimental Procedure

2.1. Synthesis

All chemicals were obtained from Sigma Aldrich (UK) and used without further purification. Choline chloride-malonic acid deep eutectic solvents were prepared in a 1:1 molar ratio and heated under stirring to 80 °C until molten and well combined. Separately a 0.5 M barium acetate solution was prepared, and 10 ml of the solution added to 10 ml of the deep eutectic solvent. The mixture was heated to 90 °C under stirring for 6 hours until all of the water had evaporated, forming a thick gel. A stoichiometric volume of titanium isopropoxide was then added under vigorous stirring. This produced a pale yellow gel which was pre-calcined in a chamber furnace in air at 500 °C for 6 hours, heated at a rate of 10 °C/min. The resulting grey pre-calcined material was spread thinly over the base of a large crucible to ensure even contact between sample and air, and calcined in air at 950 °C for 1 hour with a heating rate of 10 °C/min.

Sintered ceramics were prepared using a 10 mm die and a uniaxial press, and sintered in air at 1250 °C for 8 hours with a heating rate of 5 °C/min to achieve maximum density which was measured using the Archimedes method.

2.2. Characterization

Phase analysis for all samples was performed using a Panalytical X'Pert X-ray diffractometer. High resolution XRD patterns for lattice parameter determination were obtained using a Stoe Cu-PSD (position sensitive detector).

Ceramics for SEM were first thermally etched at 90 % of the sinter temperature for 30 minutes. The calcined powders and sintered, thermally etched ceramics were affixed to carbon pads, sputtered with gold, and imaged using a Phillips Inspect F. Energy dispersive X-ray analysis was performed using an EDAX EDS detector.

Infrared spectroscopy was performed using a Perkin Elmer Frontier FTIR and GoldenGate Diamond ATR between 4000-400 cm^{-1}. Samples for FTIR were dried at 180 °C for 24 h before testing to remove surface H_2O and CO_2. Measurements were taken with the CO_2/H_2O suppression off, which resulted in some noise in the data (2500- 1250 cm^{-1}).

Raman spectroscopy was performed using a Renishaw inVia Raman microscope with a 514 nm green laser operated at 20 mW.

Gold paste electrodes were applied to sintered ceramics for electrical testing. Bulk capacitance and tan δ (the dissipation factor expressed as the ratio of equivalent series resistance to capacitive resistance) were measured using an LCR meter (Model 4284A, Hewlett Packard, HP). Measurements were taken at the following fixed frequencies: 100 kHz, 250 kHz and 1 MHz at temperatures between 25 and 250 °C.

3. Results and discussion

The synthetic method described in the experimental section has several advantages over the traditional solid-state route. Firstly, the processing time is greatly reduced. Solid-state processing requires sieving, drying, and milling steps, often over the course of several days or weeks, in addition to high temperature calcination. The DES method negates the need for many of these steps, with the finely-grained product forming rapidly during the second heating step.

Moreover, the solid-state calcination for $BaTiO_3$ is usually performed at 1150 °C for 6 hours, followed by sintering at 1350 °C for 8 hours.[28] By comparison, the DES method used in this study, required calcination at 500 °C and 950 °C and sintering at 1250 °C to give 91 ± 1 % of the theoretical maximum density. Although this density is less than that obtained from conventional micron sized $BaTiO_3$, powders it is nonetheless in excess of previously reported densities for $BaTiO_3$ ceramics created from nanoscale powders at this temperature,[13] and could potentially be improved with further processing.

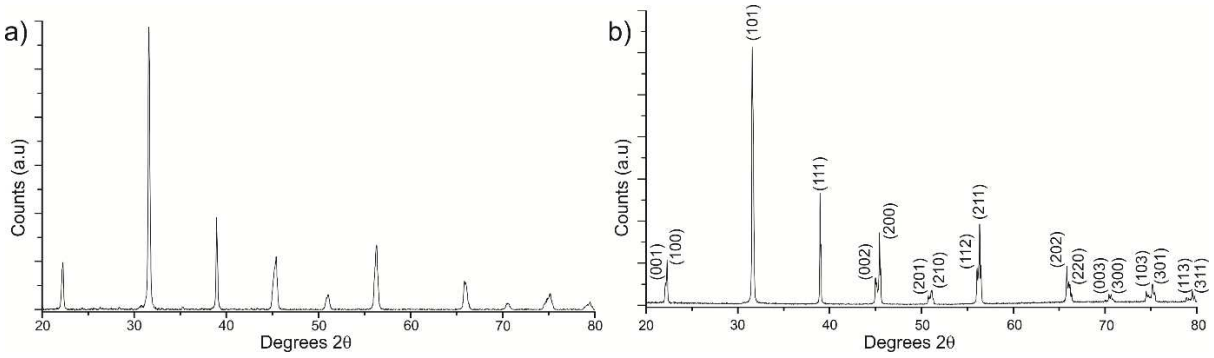

Figure 1. XRD patterns for a) calcined powder, and b) a sintered ceramic indexed to a tetragonal cell.

All peaks in the XRD traces from powder prepared using the DES method could be indexed as perovskite, as shown in Figure 1 but the tetragonal splitting is not well resolved in the calcined powder and samples appear pseudocubic. The tetragonal nature of the samples was however, confirmed by Raman spectra (Figure 2, 950 °C spectrum) which had characteristic modes associated with ferroelectric order and tetragonal symmetry at 305 cm^{-1} (the E(TO) modes) and 719 cm^{-1} (A_1(LO) phonon modes).[28] In contrast, XRD traces from crushed sintered ceramics were fully indexed on a tetragonally distorted perovskite cell, Figure 1b, with a *c/a* ratio = 1.006 ± 0.0003. The c/a ratio is commensurate within error to that associated with conventionally sintered barium titanate which suggests any residual Cl^-, NH_4^+, or OH^- ions from the DES synthesis are either removed in the gaseous phase during

calcination/sintering or have little effect on the lattice parameters and scale length of ferroelectric order.

XRD and Raman spectroscopy were also used to elucidate the synthesis pathway taken to form barium titanate using the DES method. XRD patterns of a series of samples heated to different temperatures are shown in Figure 3. At 300 °C the first crystalline phases appear, and although identification has not been possible, they are likely to be caused by crystalline metal-organic materials. The first identifiable crystalline phase to appear is barium chloride, as might be expected from the composition of the solvent and precursors, which is observed in a sample heat treated at 400 °C. Titanium emerges in a crystalline phase as anatase TiO_2 at around

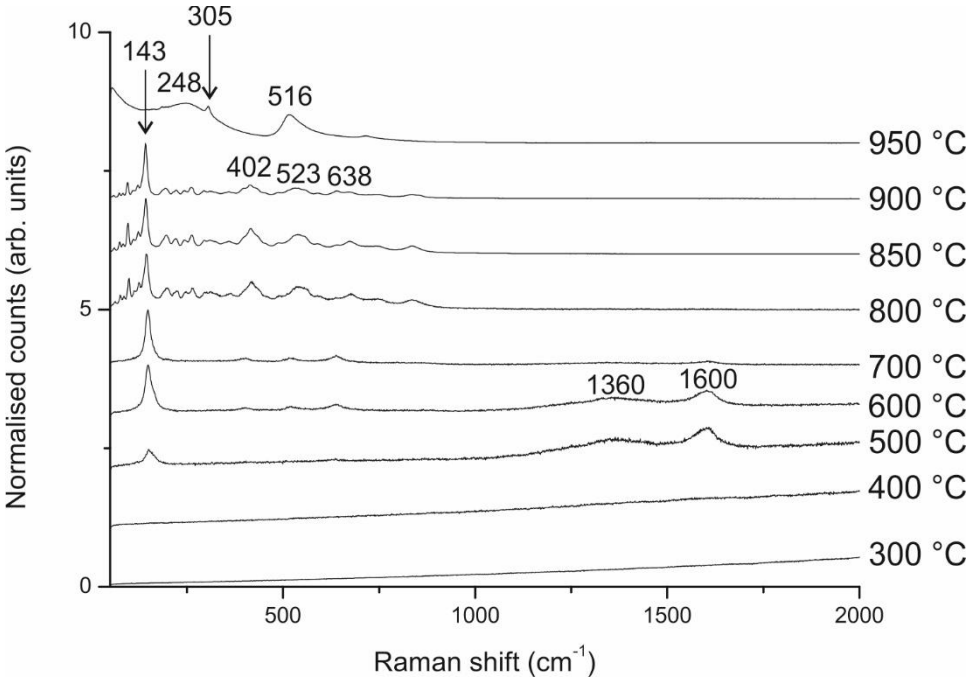

Figure 2. Raman spectra of $BaTiO_3$ powder calcined to different temperatures as indicated. The sample calcined to 950 °C shows the peak indicative of tetragonal splitting at 305 cm^{-1}.

500 °C. This is confirmed by both the XRD and Raman spectroscopy (Figure 2), with the appearance of peaks at 25.3 ° 2θ in the XRD diffractogram and 143 cm^{-1} (E_g mode) in the Raman spectrum.[30] The other indicative Raman active peaks for anatase TiO_2 at 402 cm^{-1} (B_{1g}), 523 cm^{-1} (A_{1g} or B_{1g}), and 638 cm^{-1} (E_g)[30] become apparent in the spectrum for a sample heated to 600 °C.[31] Two further peaks also appear in the Raman spectra of 600 and 700 °C heated

samples, attributed to the E_{2g} optical mode (broad, 1600 cm^{-1}) and D-band (broad, 1360 cm^{-1}) modes often observed in carbon-based materials.[32] Since their emergence is concurrent with the first crystalline phases in the XRD (Figure 3), it is concluded there is combustion of the organic matrix. The $BaCl_2$ and TiO_2 intermediates make up the principal components of the reaction mixture until 800 °C, at which point a $BaTi_5O_{11}$ phase starts to emerge in the XRD data (Figure 3). This is reflected in the Raman spectra for samples heated to 800 °C with the appearance of peaks attributed to the $BaTi_5O_{11}$ phase[33] at 93 cm^{-1}, between 200-360 cm^{-1}, and between 750-1000 cm^{-1}. The formation of such a Ti-rich binary BaO-TiO_2

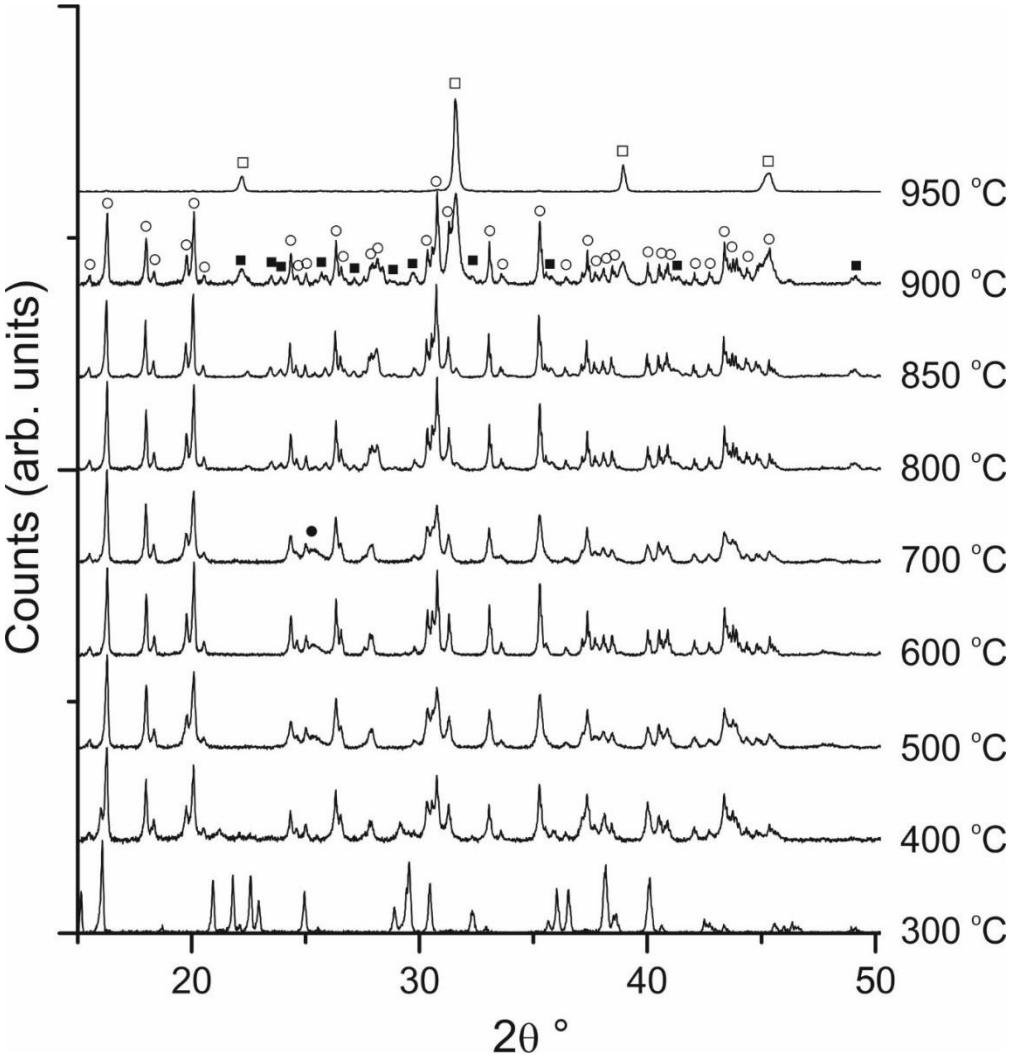

Figure 3. XRD patterns of samples calcined at intermediate temperatures between 300 and 950 °C. Compounds indexed as follows: $BaTiO_3$ (□), TiO_2 (●), $BaTi_5O_{11}$ (■), and $BaCl_2$ (O).

phase indicates the $BaCl_2$ phase is starting to react with the TiO_2, most likely through migration of the barium ions into the titanium dioxide phase. This is surprising as the anatase form of TiO_2 has been shown to be one of the slowest forms of TiO_2 to react under hydrothermal conditions.[34] That the reaction occurs so rapidly suggests the TiO_2 is readily able to allow diffusion of Ba ions into the lattice to form the Ti-rich intermediate phases. It should be noted, however, that this Ti-rich phase is likely to be transient and may only appear as a distinct crystalline phase upon cooling of the reaction mixture part way through the heating process. As the temperature increases further, and more of the Ba ions diffuse into the Ti-rich phases, perovskite $BaTiO_3$ emerges. $BaTiO_3$ is first observed in the XRD data as a very minor component phase in samples heat treated at 850 °C but is the sole phase from heat treatment at 950 °C. The Raman spectrum for samples heat treated at 950 °C reveals a typical profile for tetragonal $BaTiO_3$, confirming the tetragonal splitting in XRD data for the powder is not well resolved.

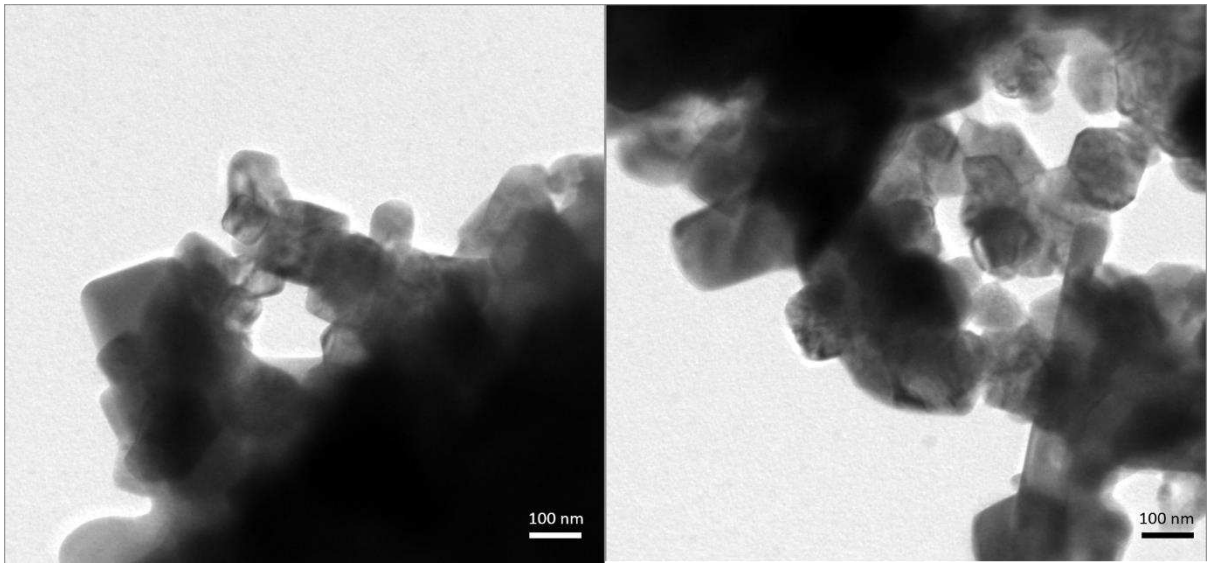

Figure 4. Representative transmission electron microscope micrographs of the calcined powder.

Transmission electron microscopy was also performed on the calcined powders (Figure 4), which gave an average particle size of 120 ± 83 nm. Scanning electron microscopy was used

to further examine the microstructure of the crystallites in the calcined powders and ceramics, Figure 5. The DES method produces a fine-grained agglomerated powder as shown in Figure 5a. Figure 5c shows the polished, thermally etched, surface of a DES pellet after sintering. The pellet has voids in the surface consistent with the measured density, and the crystallites are small. Particle size estimates show the sintered ceramics have a bimodal distribution, with roughly 25 % of the particles being of the order 0.6 ± 0.2 µm and the other 75 % being of the order 3.2 ± 1.0 µm. Energy dispersive X-ray analysis of the DES-method powder (Figure 5b)

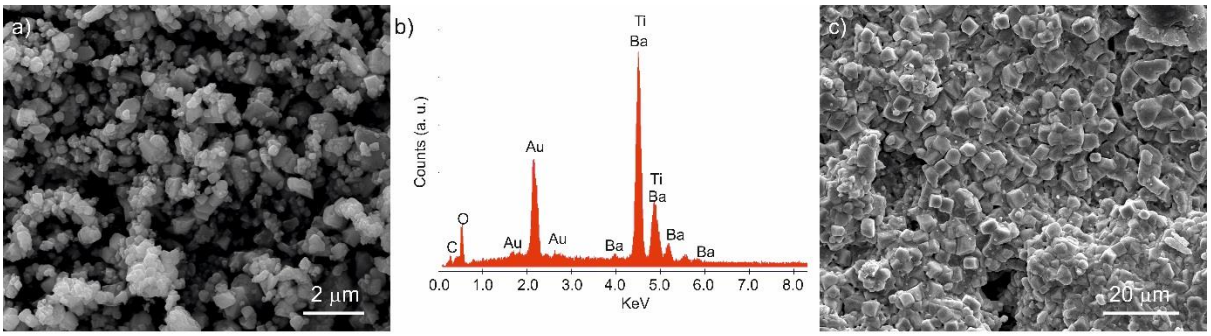

Figure 5. SEM images of a) the calcined $BaTiO_3$ powder, b) the corresponding EDXA spectrum of the calcined powder, and c) a thermally etched sintered ceramic fabricated using the $BaTiO_3$ powder.

did not the reveal the presence of any contaminant ions, suggesting the Cl ions are either eradicated during calcination or their concentration is below the detection limit of the EDS system.

The relative permittivity (ε_r) and dielectric loss (tan δ) from 25 to 225 °C are shown in Figure 6, with a large dielectric anomaly (permittivity maximum) at ~ 112 °C. This is the tetragonal-to-cubic polymorphic phase transition, T_c, which normally occurs at ~ 120 °C in coarse-grained, undoped barium titanate.[1] The occurrence of a lower T_c is unexpected given the similar *c/a* ratio of the DES method and conventional $BaTiO_3$ ceramics. Infrared spectroscopy (Figure 7) showed no evidence of a characteristic O-H stretch mode at 3480 cm^{-1} in either the calcined powder or sintered ceramics and therefore retention of hydroxyl groups in

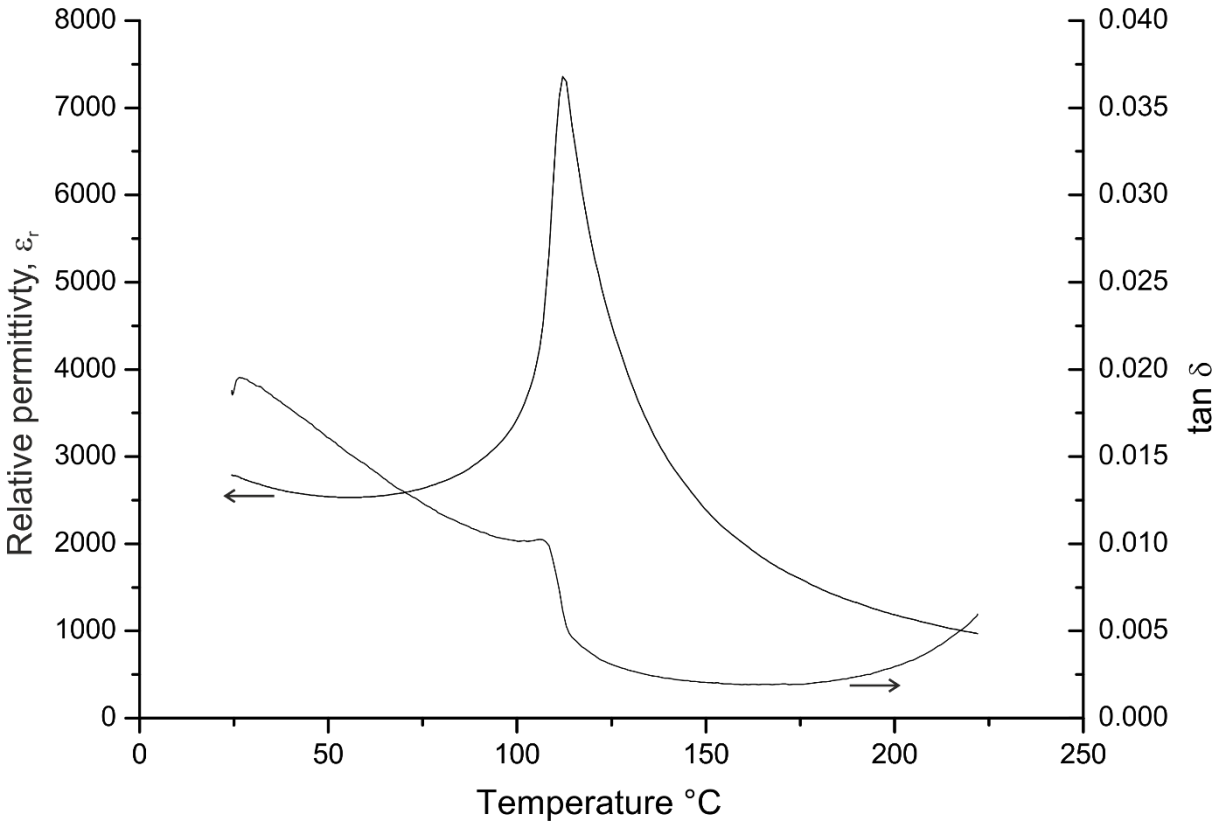

Figure 6. Relative permittivity and dielectric loss versus temperature for the DES $BaTiO_3$ sintered ceramic.

the $BaTiO_3$ lattice from the DES ceramics cannot explain the lower T_c.[35] The slight depression observed here is not detrimental to the wider use of this technique, as phase-pure barium titanate is rarely used in applications due to the large dependence of permittivity on temperature. More often, $BaTiO_3$ is combined with dopants to flatten and stabilise the temperature response,[36]

An unambiguous explanation for the lower T_c observed here is not evident and this phenomenon remains under investigation; however, it is likely, given the high concentration of chloride ions in the initial reaction mixture that small quantities of Cl^- ions are still present

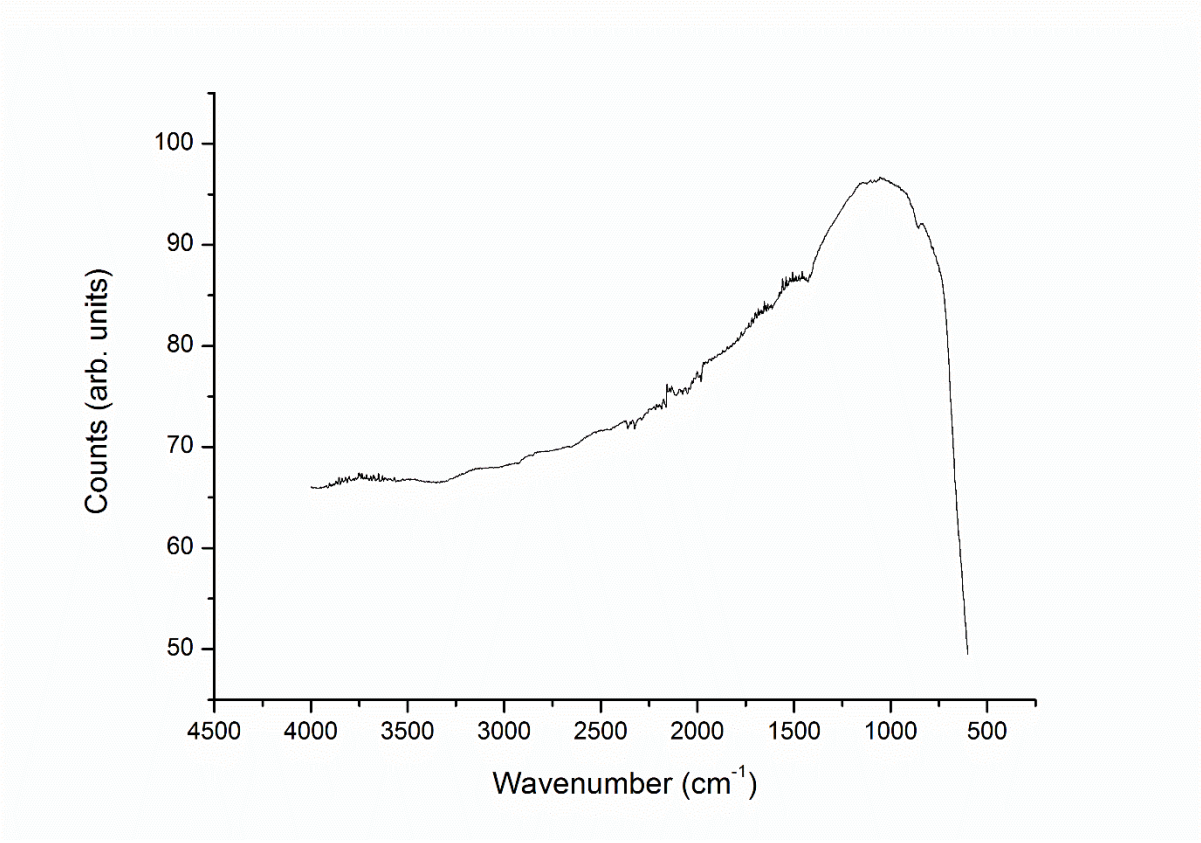

Figure 7. FTIR spectroscopy of the calcined DES powder which shows no characteristic stretch at 3480 cm^{-1} which would be expected if OH^- groups were present in the lattice.

as contaminants, residual from the synthesis but below the detection limit of the characterisation equipment used. It is unlikely, given the size of the particles measured, that the much debated strain effects are responsible for the depressed T_c, as the particles are too large to correlate with data from previous size effect studies.[37,38] The size effect in $BaTiO_3$ is also usually coupled with a reduction in the *c/a* ratio, which is not observed here.[38] It is also noteworthy that the dielectric loss, Figure 6, is higher in DES ceramics, suggesting that the defect chemistry (e.g. some substitution of Cl on the O sites) may be different to that of micron grain-sized $BaTiO_3$ ceramics prepared by conventional solid state reaction.[37]

4. Conclusions

A proof of concept study for a novel and rapid synthetic route to produce nanoscale barium titanate using a choline chloride/malonic acid deep eutectic solvent has been presented. The synthetic pathway was examined and found to progress through the formation of barium

chloride which reacts with anatase to give a final $BaTiO_3$ phase at >850 °C. The DES ceramics showed close to the expected properties for conventional solid state barium titanate ceramics. The slight depression of T_c remains under investigation, however, at this early stage of optimisation the decrease in time and energy costs afforded by this synthesis is very encouraging and deserves further investigation. The DES method is versatile and easily applicable to other oxides, particularly multicomponent systems and could be used to make chemically homogeneous, nanoscale versions of complex solid solutions such as $x(BiZn_{½}Ti_{½}O_3).(1-x)(BaTiO_3)$[9] or $x(NaNbO_3).(1-x)(BaTiO_3)$[39] for potential high temperature capacitor applications. The method circumvents the issue of poor mixing of oxide or carbonate precursors in conventional mixed oxide routes, with starting materials being homogeneously distributed from the outset. Additionally, this method can be combined with biotemplates, opening up the possibility of creating bespoke morphologies in technologically useful oxides such as titanates in a way which has not been previously accessible, and may prove extremely useful in emergent technologies such as the Cold Sintering Process.[14] Finally, the DES route offers a sustainable, low temperature route for the synthesis of a potentially wide range of advanced ceramics.

5. Acknowledgements

The authors acknowledge the EPSRC grant Sustainability and Substitution of Functional Materials and Devices (EP/L017563/1). RB thanks Dr Simon Hall for the helpful discussions.

6. References

(1) Hippel, A. Ferroelectricity, Domain Structure, and Phase Transitions of Barium Titanate. *Rev. Mod. Phys.* **1950**, *22*, 221-237.

(2) Kwei, G. H.; Lawson, A. C.; Billinge, S. J. L.; Cheong, S. W. Structures of the Ferroelectric Phases of Barium Titanate. *J. Phys. Chem.* **1993**, *97*, 2368-2377.

(3) Arlt, G.; Hennings, D.; With, G. De; Dielectric Properties of Fine-Grained Barium Titanate. *J. Appl. Phys.* **1985**, *58*, 1619-1625.

(4) Pithan, C.; Hennings, D.; Waser, R.; Progress in the Synthesis of Nanocrystalline $BaTiO_3$ Powders for MLCC. *Int. J. Appl. Ceram. Technol.* **2005**, *2*, 1-14.

(5) Takeda, H.; Aoto, W.; Shiosaki, T.; $BaTiO_3$-$(Bi_{1/2}Na_{1/2})TiO_3$ Solid Solution Semiconducting Ceramics with T_c>130 °C. *Appl. Phys. Lett.* **2005**, *87*, 102104.

(6) Raengthon, N.; Sebastian, T.; Cumming, D.; Reaney, I. M.; Cann, D. P.; $BaTiO_3$-$Bi(Zn_{1/2}Ti_{1/2})O_3$-$BiScO_3$ Ceramics for High Temperature Capacitor Applications *J. Am. Ceram. Soc.* **2012**, *95*, 3554.

(7) Morrison, F. D.; Sinclair, D. C.; West, A. R.; Electrical and Structural Characteristics of Lanthanum-Doped Barium Titanate Ceramics. *J. Appl. Phys.* **1999**, *86*, 6355-6366.

(8) Wang, D.; Khesro, A.; Murakami, S.; Feteira, A.; Zhao, Q.; Reaney, I. M. Temperature Dependent, Large Electromechanical Strain in Nd-doped $BiFeO_3$-$BaTiO_3$ Lead-free Ceramics, *J. Euro. Ceram. Soc.* **2016**, *in press.*

(9) Triamnak, N.; Yimnirun, R.; Pokorny, J.; Cann, D. P.; Relaxor Characteristics of the Phase Transformation in $(1-x)BaTiO_3$-$xBi(Zn_{1/2}Ti_{1/2})O_3$ Perovskite Ceramics. *J. Am. Ceram. Soc.* **2013**, *96*, 3176-1382.

(10) Dyer, M. S.; Collins, C.; Hodgeman, D.; Chater, P. A.; Demont, A.; Romani, S.; Sayers, R.; Thomas, F. M.; Claridge, J. B.; Darling, G. R.; Rosseinsky, M. J.; Computationally Assisted Identification of Functional Inorganic Materials. *Science* **2013**, *340*, 847-852.

(11) Nagata, H.; Yoshida, M.; Makiuchi, Y.; Takenaka, T.; Large Piezoelectric Constant and High Curie Temperature of Lead-Free Piezoelectric Ceramic Ternary System Based on Bismuth Sodium Titanate-Bismuth Potassium-Barium Titante Near the Morphotropic Phase Boundary. *Jpn. J. Appl. Phys.* **2003**, *42*, 7401-7403.

(12) Kishi, H.; Okino, Y.; Honda, M.; Iguchi, Y.; Imaeda, M.; Takahashi, Y.; Ohsato, H.; Okuda, T. The Effect of MgO and Rare-Earth Oxide on Formation Behavior of Core-Shell Structure in $BaTiO_3$. *J. Am. Ceram. Soc.* **1997**, *36*, 5954-5957.

(13) Buscaglia, M. T.; Bassoli, M.; Buscaglia, V. Solid-State Synthesis of Ultrafine $BaTiO_3$ Powders from Nanocrystalline $BaCO_3$ and TiO_2. *J. Am. Ceram. Soc.* **2005**, *88*, 2374-2379.

(14) Guo, J.; Guo, H.; Baker, A. L.; Lanagan, M. T.; Kupp, E. R.; Messing, G. L.; Randall, C. A. Cold Sintering: A Paradigm Shift for Processing and Integration of Ceramics. *Angew. Chem.* **2016**, *128*, 11629-11633.

(15) Komarneni, S.; Abothu, I. R..; Rao, A. V. P. Sol-Gel Processing of Some Electroceramic Powders. *J. Sol-Gel Sci. Technol.* **1999**, *15*, 263-270.

(16) Kareiva, A.; Tautkus, S; Rapalaviciute, R.; Jørgensen, J. -E.; Lundtoft, B. Sol-Gel Synthesis and Characterization of Barium Titanate Powders. *J. Mater. Sci.* **1999**, *34*, 4853-4857.

(17) Takeuchi, T.; Suyama, Y.; Sinclair, D. C.; Kageyama, H. Spark-Plasma-Sintering of Fine $BaTiO_3$ Powder Prepared by a Sol-Crystal Method. *J. Mater. Sci.* **2001**, *36*, 2329-2334.

(18) Schnepp, Z. Biopolymers as a Flexible Resource for Nanochemistry. *Angew. Chem. Int. Ed.* **2013**, 52, 1096-1108.

(19) Walsh, D.; Wimbush, S. C.; Hall, S. R. Use of the Polysaccharide Dextran as a Morphological Directing Agent in the Synthesis of High-T_c Superconducting

$YBa_2Cu_3O_{7-\delta}$ Sponges with Improved Critical Current Densities. *Chem. Mater.* **2007**, *19*, 647-649.

(20) Cung, K.; Han, B. J.; Nguyen, T. D.; Mao, S.; Yeh, Y. -W.; Xu, S.; Naik, R. R..; Poirier, G.; Yao, N.; Purohit, P. K.; McAlpine, M. C. Biotemplated Synthesis of PZT Nanowires. *Nano Lett.* **2013**, *13*, 6197-6202.

(21) Green, D. C.; Glatzel, S.; Collins, A. M.; Patil, A. J.; Hall, S. R. A New General Synthetic Strategy for Phase-Pure Complex Functional Materials. *Adv. Mater.* **2012**, *24*, 5767-5772.

(22) Abo-Hamad, A.; Hayyan, M.; AlSaadi, M. A.; Hashim, M. A. Potential Application of Deep Eutectic Solvents in Nanotechnology. *Chem. Eng. J.* **2015**, *273*, 551-567.

(23) Smith, L. E.; Abbott, A. P.; Ryder, K. S. Deep Eutectic Solvents (DESs) and Their Applications. *Chem. Rev.* **2014**, *114*, 11060-11082.

(24) Abbott, A. P.; Boothby, D.; Capper, G.; Davies, D. L.; Rasheed, R. K. Deep Eutectic Solvents Formed Between Choline Chloride and Carboxylic Acids: Versatile Alternatives to Ionic Liquids. *J. Am. Chem. Soc.* **2004**, *126*, 9142-9147.

(25) Schnepp, Z. A. C.; Wimbush, S. C.; Mann, S.; Hall, S. R. Structural Evolution of Superconductor Nanowires in Biopolymer Gels. *Adv. Mater.* **2008**, *20*, 1782-1786.

(26) Abbott, A. P.; Frisch, G.; Hartley, J.; Ryder, K. S. Processing of Metals and Metal Oxides Using Ionic Liquids. *Green Chem.* **2011**, *13*, 471-481.

(27) Abbott, A. P.; Capper, G.; Davies, D .L.; McKenzie, K. J.; Obi, S. U. Solubility of Metal Oxides in Deep Eutectic Solvents Based on Choline Chloride. *J. Chem. Eng. Data* **2006**, *51*, 1280-1282.

(28) Zhou, L.; Vilarinho, P. M.; Baptista, J. L. Dependence of the Structural and Dielectric Properties of $Ba_{1-x}Sr_xTiO_3$ Ceramic Solid Solutios on Raw Materials Processing *J. Eur. Ceram. Soc.* **1999**, *19*, 2015-2020.

(29) Zhang, W.; Chen, L.; Jin, C.; Deng, X.; Wang, X.; Li, L. High Pressure Raman Studiesof Dense Nanocrystalline $BaTiO_3$ Ceramic. *J. Electroceramics* **2008**, *21*, 859-862.

(30) Zhang, W. F.; He, Y. L.; Zhang, M. S.; Yin, Z.; Chen, Q. Raman Scattering Study on Anatase TiO_2 Nanocrystals. *J. Phys. D. Appl. Phys.* **2000**, *33*, 912-916.

(31) Felske, A.; Plieth, W. J. Raman Spectroscopy of Titanium Dioxide Layers. *Electrochim. Acta* **1989**, *34*, 75-77.

(32) Tuinstra, F.; Koenig, L. Raman Spectrum of Graphite. *J. Chem. Phys.* **1970**, *53*, 1126-1130.

(33) Yamashita, Y.; Tada, M.; Kakihana, M.; Osada, M.; Yoshida, K. Synthesis of RuO_2-Loaded $BaTi_nO_{2n+1}$ (n = 1, 2 and 5) Using a Polymerizable Complex Method and its Photocatalytic Ability for the Decomposition of Water. *J. Mater. Chem.* **2002**, *12*, 1782-1786.

(34) Clark, I. L.; Takeuchi, T.; Ohtori, N.; Sinclair, D. C. Hydrothermal Synthesis and Characterisation of $BaTiO_3$ Fine Powders: Precursors, Polymorphism and Properties. *J. Mater. Chem.* **1999**, *9*, 83-91.

(35) Jovanović, A.; Wöhlecke, M.; Kapphan, S.; Maillard, A.; Godefroy, G. Infrared Spectroscopy of Hydrogen Centres in Undoped and Iron-Doped $BaTiO_3$ Crystals. *J. Phys. Chem. Solids* **1989**, *50*, 623-627.

(36) Dean, J.; Foeller, P. Y.; Reaney, I. M.; Sinclair, D. C. A Resource Efficient Design Strategy to Optimise the Temperature Coefficient of Capacitance of $BaTiO_3$-Based Ceramics using Finite Element Modelling. *J. Mater. Chem. A* **2016**, *4*, 8696-6901.

(37) Frey, M. H.; Xu, Z.; Han, P.; Payne, D. A. The Role of Interfaces on an Apparent Grain Size Effect on the Dielectric Properties or Ferroelectric Barium Titanate Ceramics. *Ferroelectrics* **1998**, *206–207*, 337-353.

(38) Zhao, Z.; Buscaglia, V.; Viviani, M.; Buscaglia, M. T.; Mitoseriu,; L.; Testino, A.; Nygren, M.; Johnsson, M.; Nanni, P. Grain-Size Effects on the Ferroelectric Behaviour of Dense Nanocrystalline $BaTiO_3$ Ceramics. *Phys. Rev. B* **2004**, *70*, 24107.

(39) Saito, Y.; Takao, H.; Tani, T.; Nonoyama, T.; Takatori, K.; Homma, T.; Nagaya, T.; Nakamura, M. Lead-Free Piezoceramics. *Nature* **2004**, *432*, 84.

For Table of Contents Only

A deep eutectic solvent of malonic acid and choline chloride has been used to synthesize ferroelectric barium titanate. The barium titanate forms at 950 °C mediated by the intermediate phases barium chloride and titanium dioxide. The materials sinter at a lower temperature than the solid state equivalent whilst retaining comparable properties. This synthesis represents a flexible and widely applicable method which can be applied to a range of functional materials to produce nanoscale powders.